Threshold Voltage Variability of NROM Memories After Exposure to Ionizing Radiation

Domenico Corso, Sebania Libertino, Michael Lisiansky, Yakov Roizin, Felix Palumbo, Fabio Principato, Calogero Pace, Paolo Finocchiaro, and Salvatore A. Lombardo

***Abstract*—Threshold voltage (V_{th}) behavior of nitride read-only memories (NROMs) was studied after irradiation with photons (γ- and X-rays), light and heavy ions. Both programmed and nonprogrammed single cells were investigated. The data suggest that two main physical phenomena are contributing to V_{th} variation and that the V_{th} loss and the variability can be modeled by a Weibull statistics with a shape parameter $k \sim 2.2$ regardless of the irradiation species and total dose. The same peculiarities were found in large memory arrays, confirming the results from single-cell studies but with significantly larger statistics. Hence, once the irradiation dose is known, the V_{th} loss distribution can be obtained, thus providing a predictive model of the radiation tolerance of NROM memory arrays.**

***Index Terms*—Flash memories, nitride read-only memories (NROMs), oxide–nitride–oxide (ONO), radiation hardness.**

I. Introduction

NONVOLATILE semiconductor memories (NVMs) are fundamental components of various electronic circuits. Most of the commercial semiconductor nonvolatile memory cells are based on charge storage in the floating gate (FG) of MOS structures. The FG is insulated from the channel and from the gate by high-quality dielectrics. The retention of the stored charge in polycrystalline Si FG NVM is limited by the intrinsic leakage currents through the dielectrics. Retention is further worsened after multiple program/erase operations due to creation of extrinsic defects in the gate dielectrics, resulting in local trap-assisted tunneling.

A successful alternative to the polycrystalline Si FG approach is the use of discrete nodes for charge storage, now approximately 25% of the code storage semiconductor NVM market. This approach is also based on a MOS transistor with an FG but employs storage of charge on traps. They are either metals or semiconductor nanocrystals (NCs) embedded into high-quality dielectrics, or native traps in thin dielectric layers, e.g., silicon/oxide/nitride/oxide/silicon (SONOS) structures with stoichiometric or silicon-rich $\mathrm{Si_3N_4}$.

The discrete storage devices allow enhanced reliability since the charge in the FG of a memory cell is immobile. The charge is stored at numerous trapping nodes. If a defect is formed in the FG surrounding dielectric, the charge loss is limited only to one or few nodes closest to the defect. The remaining nodes maintain their charge state, and thus, the information is preserved. These features contribute to the immunity of the device to electrical stress and ionizing radiation, both having a pronounced effect on the NVM charge retention.

The need to use NVM in avionics, space, and other radiation-hardness-requiring applications stimulated corresponding research studies. Many different memory principles and architectures were tested for ionizing radiation hardness: FG memory devices [1]–[3], NC NVM [4], [5], and nitride read-only memories (NROMs) [6], [7].

NROMs are based on SONOS structures [8]. The features of an NROM device are shown in the inset of Fig. 1. Unlike the traditional SONOS, the oxide–nitride–oxide (ONO) stack of NROM is designed with thicker bottom oxide to ensure retention and suppress read disturbs [9], [10]. The memory bit is programmed by channel-hot-electron injection: Electrons are injected into the ONO regions aligned to the metallurgical junctions and trapped in the nitride layer. The trapped charge package is strongly localized in a region of ~20 nm in length [11] at the transistor channel edges (see the inset, locations bit 1 and bit 2). The strong localization allows one to program also the other end of the channel as an independent bit, thus enabling the storage of 2 b/cell. The read operation is performed by applying a low voltage (usually 1.2–1.8 V) in the opposite direction with respect to the programming current (see the inset of Fig. 1, arrows for programming and reading bit 1) [8]. The typical device drain–source current–gate voltage (I_{DS}–V_G) characteristics for bit 1 are shown in Fig. 1 for the different device states: fresh (black dotted–dashed line), programmed (blue solid line), and erased (red dotted line). The threshold voltage (V_{th}) here is defined as the gate voltage at

Manuscript received February 7, 2012; revised May 21, 2012; accepted June 25, 2012. Date of publication August 24, 2012; date of current version September 18, 2012. This work was supported by “con il contributo del Ministero degli Affari Esteri, Direzione Generale per la Promozione del Sistema Paese,” through the Progetto di Grande Rilevanza Italia–Argentina “Caratterizzazione durante e post-irraggiamento di dispositivi microelettronici per applicazioni avioniche o spaziali.” The review of this paper was arranged by Editor H. Shang.

D. Corso, S. Libertino, and S. A. Lombardo are with the Istituto per la Microelettronica e Microsistemi, National Council of Research (CNR), 95121 Catania, Italy (e-mail: domenico.corso@imm.cnr.it; sebania.libertino@imm.cnr.it; salvatore.lombardo@imm.cnr.it).

M. Lisiansky and Y. Roizin are with Tower Semiconductor, Migdal Haemek 23105, Israel (e-mail: michaelx@towersemi.com; yakovro@towersemi.com).

F. Palumbo is with the Consejo Nacional de Investigaciones Científicas y Técnicas–Comision Nacional de Energia Atomica, Buenos Aires 1650, Argentina (e-mail: palumbo@cnea.gov.ar).

F. Principato is with the Department of Physics, University of Palermo, 90128 Palermo, Italy (e-mail: fabio.principato@unipa.it).

C. Pace is with the Department of Electronics, Computer Science and Systems, University of Calabria, 87036 Rende, Italy (e-mail: cpace@unical.it).

P. Finocchiaro is with the Laboratori Nazionali del Sud, Istituto Nazionale di Fisica Nucleare, 95100 Catania, Italy (e-mail: finocchiaro@lns.infn.it).

Color versions of one or more of the figures in this paper are available online at http://ieeexplore.ieee.org.

Digital Object Identifier 10.1109/TED.2012.2206596

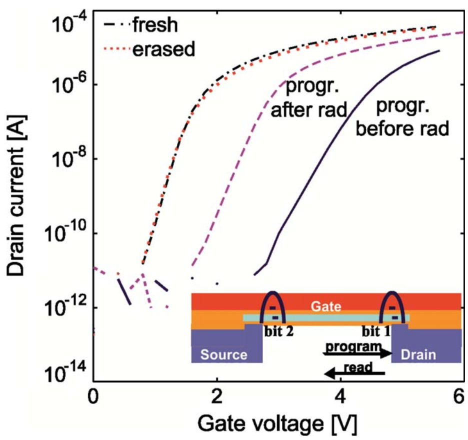

Fig. 1. Drain–source current as a function of the gate voltage (black dotted–dashed line) for a fresh bit, (blue solid line) after programmed, (red dotted line) after erase, and (magenta dashed line) after irradiation with 10-MeV B to a dose of 580 krd(Si). In the inset, a schematic view of device operation (the charge stored at the junction edges) and the (arrows) programming/reading conditions for bit 1.

$I_{\rm DS} = 1\ \mu$A, and a clear $V_{\rm th}$ shift is evident in Fig. 1. The erase operation is performed by band-to-band-tunneling-assisted hot hole injection. Also, holes are locally injected into the regions close to the metallurgical junctions, where the electron charge is stored. As a result of the erase operation, the device I–V curve returns to the non-programmed state.

NROM memories were shown to have major advantages over polycrystalline Si FG memories from the radiation immunity point of view. Since the volume where the charge is trapped is very small, the probability to create a leakage path from this volume is low. Moreover, even if such a leakage path is created, only a very limited number of trapped charge carriers are lost: in NROM, unlike in polycrystalline Si FG memories, lateral charge migration is strongly suppressed. For moderate total absorbed doses (e.g., below 100 krd of γ-radiation), the main effect is trapping of holes generated by ionizing radiation within, or in proximity of, the ONO, which leads to the $V_{\rm th}$ loss.

In this paper, we demonstrate that the statistics of $V_{\rm th}$ loss in the NROM NVM cells and arrays after irradiation has some very general features, independent of the dose and the type of radiation. Several ionizing radiation sources were used (light and heavy ions; γ- and X-ray photons) featuring different energy loss mechanisms in the device. We suggest a physical explanation for the $V_{\rm th}$ loss and provide a simple model to fit all the experimental data.

II. Experiment

NROM cells were manufactured in Tower Semiconductor Ltd. (microflash process flow) with channel dimensions of $W \times L = 0.18 \times 0.42\ \mu{\rm m}^2$. They are also used in 4–8-Mb embedded memory modules. Only 1 b/cell was programmed. This was done by applying a gate voltage (V_G) of 9 V and a drain voltage (V_D) of 4 V for 10 μs. Erase was achieved by applying $V_D = 9$ V and source voltage $(V_S) = 3$ V, at $V_G = 0$ V for 50 ms. Readout was performed at $V_{\rm DS} = 1.8$ V. The $V_{\rm th}$ was measured at a drain current $(I_{\rm DS})$ of 1 μA. Although the investigated NROM memories were capable to store 2 b/cell, the option to program only 1 b was chosen in order to maximize the sensitivity to lateral charge motion. Lateral charge migration (spread of locally trapped charges) is one of the dominant mechanisms responsible for $V_{\rm th}$ decrease of programmed NROM cells.

Both single cells and memory arrays were irradiated at room temperature in dark conditions with floating electrodes, using either γ- or X-ray photons or high-energy ions. The irradiation details are summarized in Table I. The calculation made basing on linear energy transfer (LET) values reported in the table does not take into account the columnar recombination effect observed in dielectrics after irradiation [12]. The effective number of charges trapped in the ONO will be much lower than that predicted by calculation without an account of columnar recombination. It should be noted that, according to [13], the difference in the fluxes was not expected to affect the results. To guarantee statistically significant results, at least ten memory cells were studied for each of the doses and types of irradiation. A total of $\sim$1000 samples was investigated. In addition to single-cell irradiation, 8-Mb arrays were used in the γ-ray experiments, enabling to investigate the radiation effects with larger statistics. To compare all the different radiation sources, the total fluence in the case of ion irradiations, measured in ions per square centimeter, was converted into absorbed dose evaluated in rd(Si) as used for the case of photon irradiations [7]. The ion energies were chosen to introduce the implanted ions (B, Br, and Au) deep into the Si substrate, beyond the device active part. This is illustrated by the ion projected ranges also reported in Table I. All cells were fully characterized before and after irradiation.

III. Results and Discussion

To understand the results presented hereinafter, the following comments should be done. The main degradation effect in NROM at moderate radiation doses, below 100 krd, is charge trapping in the memory stack. Once high-energy electron/hole pairs are generated by the ionizing radiation, the electrons escape the dielectric stack [14] while the holes can be captured by silicon nitride or oxide traps. At higher radiation doses, the effects connected with defect creation in the oxide layers may become pronounced, leading to creation of clusters of traps that can act as percolation paths. These effects are particularly pronounced in the ONO bottom oxide where even one trap in the middle of 5-nm bottom oxide would result in a percolation path (leakage channel).

A. Single Cells

The effects of irradiation were observed by monitoring $V_{\rm th}$ before $(V_{\rm th}^i)$ and after $(V_{\rm th}^f)$ irradiation. An example of $V_{\rm th}$ shift after irradiation is shown in Fig. 1 (magenta dashed line) in the case of 10-MeV B irradiation to a dose of $\sim$580 krd, corresponding to 1×10^{10} ions/cm^2. The shift indicates a partial compensation of the electron charge at nitride traps. The $V_{\rm th}$ difference, reported as $\Delta V_{\rm th} = V_{\rm th}^f - V_{\rm th}^i$, was recorded as a function of the total irradiation dose for the different irradiation sources. The results for programmed bits are summarized in

TABLE I
LIST OF THE SPECIES IRRADIATED AND DETAILS OF IRRADIATION (WHERE APPLICABLE): ENERGY, DOSE (Φ), DOSE RATE, PROJECTED RANGE (R_P), STRAGGLING (ΔR_P), LET, AND ABSORBED DOSE ($DOSE_{\rm ABS}$) IN krd(Si)

Species	E [MeV]	Φ [cm^{-2}]	Dose rate	Rp [µm]	ΔRp [µm]	LET [MeV/mg/cm^2]	$DOSE_{abs}$ [krad(Si)]
γ-rays (^{60}Co)	~1.25	-	3.6 rad(Si)/s				9.4–52
X-rays (W–L lines)	~0.010	-	3.9 rad(Si)/s				3–100
^{11}B	10	10^8–5×10^{10}		12	0.2	3.5	5.8-2900
^{79}Br	196	5×10^8–10^{11}		26.4	0.6	38.8	255-51040
^{197}Au	5100	10^9–5×10^{10}		291	1.1	64.4	1200-60190

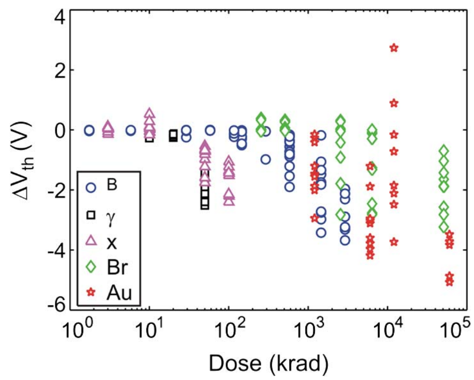

Fig. 2. Threshold voltage shift as a function of the log of the irradiation dose for programmed bits after (black squares) γ-rays, (magenta triangles) X-rays, (blue circles) B, and (green diamonds) Br and (red stars) Au irradiations.

Fig. 2 for all the experiments performed (the data points of non-programmed bits are not reported to avoid figure overload). Three main features are immediately observed regardless of the irradiation source: 1) The average $|\Delta V_{\rm th}|$ increases with the irradiation dose; 2) a noticeable $\Delta V_{\rm th}$ dispersion is observed for all the experiments, and it increases with the dose; and 3) only a small percentage of samples shows increased $V_{\rm th}$ (higher negative charge) after irradiation. We argue that positive $V_{\rm th}$ shifts are connected with trapping statistics of the generated by radiation electrons and holes. Holes are easily trapped in oxides (mostly at the periphery of the NROM transistors). Trapping of holes usually dominates over the trapping of electrons. Moreover, electrons are repulsed from the negatively charged nitride regions in ONO. Nevertheless, statistically, in rare occasions, an opposite effect can be observed (for programmed cells, the hot electrons generated by radiation overcome the energy barrier in programmed cells). In the rest of this paper, only negative $V_{\rm th}$ shifts (trapping of holes) are discussed.

Strong charge recombination effects during ion irradiation can be assumed when analyzing the data in Fig. 2. The same $V_{\rm th}$ loss is observed after 50-krd X-ray irradiation and 580-krd B irradiation. According to Oldham [12], most of the charges deposited in the dielectric by ion irradiation recombine, leaving only a small residual amount of charges to be trapped. The estimates show that the fraction of charges that can be trapped is about a factor ten lower for B irradiation compared with photon (gamma) irradiation. The ratio is higher when the ion mass increases, as observed after Br or Au irradiations.

To better understand the statistics of the charge loss ($\Delta V_{\rm th}$), the standard deviation ($\sigma_{\Delta V{\rm th}}$) of $\Delta V_{\rm th}$ was plotted as a function of the average $\Delta V_{\rm th}$ ($\mu_{\Delta V{\rm th}}$) for all the experiments that we carried out. Both programmed and second (non-programmed) bits were measured, and the results are shown in Fig. 3(b) and (a), respectively. Second bit results show initial negative charging of ONO stack at the end of line (in the end of process flow). Fig. 3(a) shows the decrease of this charge during irradiation (the $V_{\rm th}$ of a dummy cell is ≤ 1 V). The data clearly indicate a unique trend: linear dependence in a log–log scale. The linear fit, shown in both figures by a solid line, has a slope of $\sim$2.1 $\pm$ 0.4, suggesting that the average (μ) and the standard deviation (σ) of the threshold voltage shift are related by

$$\mu_{\Delta V{\rm th}} \cong 2.1\sigma_{\Delta V{\rm th}}. \tag{1}$$

The exact matching of slopes for programmed and second bit hints to the same origin of the charge loss regardless of the stored amount of charge. Although, for each single radiation type and dose, the sample size is not large, numerous sets of radiation sources and doses spanning over many decades demonstrate the same trend for programmed and second bits as well: all the measurement points fall onto the same line (Fig. 3(b) and 3(a), respectively). Thus, we conclude that (1) holds regardless of the amount of stored charge, radiation type, and dose, including ^{60}Coγ-rays from a few kilorads to more than 60 Mrd with Au ions having energies of $\sim$5 GeV. The data, therefore, strongly suggest that a common physical phenomenon is the root cause of the observed trend.

We now discuss the possible reasons for such a result. It is well known that the ionizing radiation damage is randomly distributed in the gate dielectrics. An example of random process ending up in the memory charge loss from the FG is the oxide dielectric breakdown [15]–[17]. Oxide breakdown phenomena are well described by the Weibull distribution, which reflects the random character of leakage path creation [18]. Radiation degradation includes random charge trapping that may be also accompanied by leakage path creation at high absorbed doses.

The Weibull function is expressed as:

$$F(x) = 1 - \exp\left[-\left(\frac{x}{\lambda}\right)^k\right]. \tag{2}$$

$F(x)$ is the cumulative failure probability, i.e., the fraction of failed devices when the number of defects in the device is equal to x, k is the shape parameter, and λ is the scale parameter of the distribution. The characteristic λ value corresponds to the x value where 63.2% of the samples fail.

The ionizing radiation will produce holes which either discharge the trapped electrons or are captured on defects and,

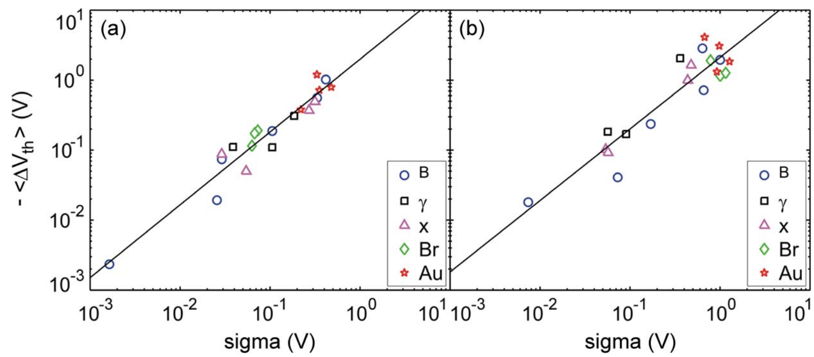

Fig. 3. Averaged threshold shift as a function of the dispersion in (a) nonprogrammed and (b) programmed bits after irradiation with (black squares) γ-rays, (magenta triangles) X-rays, and (blue circles) B, (green diamonds) Br, and (red stars) Au irradiations.

therefore, locally compensate the charge of the trapped electrons. Let us consider that, for each discharged or compensated electron, the $\Delta V_{\rm th}$ is equal N times $\Delta V_{\rm th0}$, where N is the number of discharged, or compensated, electrons and $\Delta V_{\rm th0}$ is $q/C_{\rm self}$, where q is the elementary charge and $C_{\rm self}$ is the self-capacitance of the storage defect. Then, if the NROM array is subjected to an irradiation to a dose D_0, each of the cells will have a $\Delta V_{\rm th} = N * \Delta V_{\rm th0}$, and we expect that:

$$F(\Delta V_{\rm th}) = 1 - \exp\left[-\left(\frac{\Delta V_{\rm th}}{\lambda}\right)^k\right]. \tag{3}$$

The average and standard deviation of the distribution are then:

$$\mu = \lambda\Gamma(1 + 1/k) \tag{4}$$

$$\sigma = \lambda \cdot \sqrt{\Gamma(1 + 2/k) - \Gamma^2(1 + 1/k)} \tag{5}$$

where Γ is the gamma function defined as $\Gamma(z) = \int_0^{+\infty} t^{z-1}e^{-1}dt$.

According to (1):

$$\Gamma(1 + 1/k) \approx 2.1 \cdot \sqrt{\Gamma(1 + 2/k) - \Gamma^2(1 + 1/k)}. \tag{6}$$

The condition expressed by (6) is satisfied only by $k \cong 2.2$ (numerically determined). Therefore, we conclude that, even if the radiation source and irradiation conditions are drastically varied, in all cases, the same k, i.e., Weibull distribution slope, should be observed in a graph of the $\ln[-\ln(1 - F)]$ against $\ln(x/\lambda)$ (Weibit).

In order to verify this hypothesis, the different collected data are compared using the same normalized scale. For this reason, for each data set, we assumed a Weibull function having $k = 2.2 \pm 0.5$ and λ determined from (4) using the experimental mean value. The Weibull cumulative distribution can be represented as a straight line by plotting the Weibit. In these coordinates, k is the slope. All our normalized experimental data are summarized in Fig. 4. The Weibull distribution with $k = 2.2$ is presented as a solid straight line. The statistical confidence of our measurements is expressed by two curves on both sides of $F(x, \lambda, k)$. The results indicate 95% confidence level for a set of ten samples (calculated according to Jacquelin [19]). It is evident that all our data points follow quite well the proposed statistics. Some points outside the confidence levels

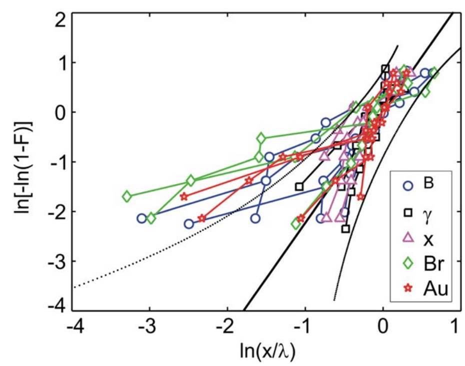

Fig. 4. (Solid black line) Weibull function with $k = 2.2$ for all the experiments performed on programmed bits with (black squares) γ-rays, (magenta triangles) X-rays, and (blue circles) B, (green diamonds) Br, and (red stars) Au irradiations. The black curves on both sides of the Weibull function indicate the 95% confidence level for a set of ten samples (after Jacquelin [19]).

(green diamonds and red downward triangles in Fig. 4) are attributed to problems with some of the devices irradiated with large Br and Au doses. Some of these transistors underwent an irreversible damage and were not included in the analysis (out of the ten-device set). In such a case, the confidence limits for the 95% confidence should be broader than those reported in Fig. 4 [19].

The analysis of irradiated single cells clearly shows that all the device sets, regardless of radiation sources and doses, belong to the same Weibull distribution. This is a direct evidence that all the results are ruled by the same physical phenomenon. It should be mentioned that, to our knowledge, it is the first time that a Weibull function is used to model the charge loss effects in NROM memory devices.

B. Memory Arrays

Results consistent with the reported observations on the single cells are provided by measurement performed on 8-Mb memory arrays for moderate irradiation doses in the range 50–200 krd (γ-rays). If our hypothesis is correct, i.e., the $\Delta V_{\rm th}$ distributions follow Weibull statistics with $k \sim 2.2$, it should be possible, by having the initial $V_{\rm th}^i$ distribution, to predict the final $V_{\rm th}^f$ distribution after irradiation. This hypothesis was verified by calculating the $V_{\rm th}^f$ distribution by the Monte Carlo method and comparing it to the experimental one. The calculated $V_{\rm th}^f$ distribution is obtained by the convolution

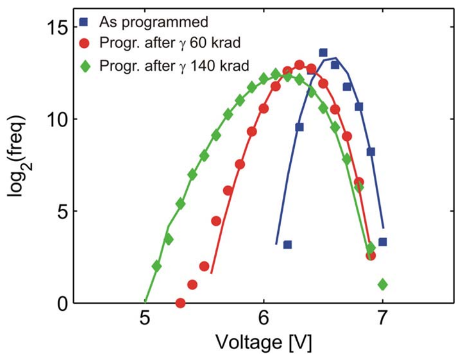

Fig. 5. Threshold voltage distribution in an 8-Mb Topaz module (blue squares) before irradiation and after irradiation with (red circles) 60-krd and (green diamonds) 140-krd γ-rays. The solid red and green lines are the Monte Carlo simulation results obtained for the two aforementioned doses, respectively, using a Weibull distribution with $k = 2.2$ and λ as the fitting parameter.

of the Gaussian V_{th}^{i} distribution (before irradiation) with a Weibull distribution [see (3)] having $k = 2.2$ and λ as the fitting parameter. Fig. 5 shows the experimentally measured V_{th} (blue squares) and V_{th}^{f} distribution after 60-krd (red circles) and 140-krd (green diamonds) γ-ray irradiations together with appropriate Monte Carlo calculated distributions (red and green lines, respectively). The agreement between the experimental data and the simulated profiles is excellent. This is an additional confirmation of the revealed dependence on a large statistical set of devices showing that, in NROM memory, the V_{th} loss under ionizing radiation exposure is defined by the same physical mechanism. The Weibull distribution with $k = 2.2$ is completely able to predict the V_{th} distribution also in large NVM arrays.

C. Physical Explanation

V_{th} loss may be due to two possible phenomena connected with hot holes generated by radiation: 1) trapping of thermalized holes or 2) creation of traps in the oxide layers. Trapped holes compensate the electron charge stored in the nitride traps. Trap-assisted tunneling generated by defects can also result in progressive discharge of the stored electrons with the increasing of radiation dose. Both phenomena can work in parallel, or one may dominate. For the first mechanism, one would expect a distribution resembling the one obtained by random shots at a "2-D rectangular target" consisting of the stored electrons in the nitride layer. The random shots follow two independent normal distributions in orthogonal directions. The relevant statistics for the charge loss is then the convolution of two normal distributions of similar variance. Such distributions are known to obey Rayleigh statistics, i.e., a Weibull distribution with $k = 2$. This value is very close to 2.2 registered in our experiments. On the other hand, electron discharge by trap-assisted tunneling is expected to dominate the V_{th} loss at high radiation doses. In this case, the mechanism of the phenomenon is similar to oxide breakdown under high field electrical stress. It is known that the breakdown statistics under constant voltage stress results in a Weibull distribution with a very similar k value for the same oxide thicknesses [16].

IV. Conclusion

In summary, the reported data have indicated that the V_{th} loss in NROM memory devices due to ionizing radiation exposure exhibits a variability well explained by a Weibull statistics with a $k \sim 2.2$ shape parameter regardless of the irradiation species, sweeping from photons of different energies (γ- and X-rays) to light (B) and heavy (Br and Au) ions, and regardless of the total dose used, ranging from a few kilorads to ~60 Mrd.

Trapping of thermalized holes and/or the creation of defect traps in the NROM oxide layers contributes to V_{th} loss. Both phenomena are well modeled by a Weibull statistics with a shape parameter $k \sim 2.2$. Also, the behavior of very large memory arrays is well explained by the aforementioned statistics. In conclusion, once the irradiation dose is known, the V_{th} loss distribution can be predicted, thus providing a forecast of the radiation tolerance of the NROM memory arrays.

References

[1] G. Cellere, A. Paccagnella, A. Visconti, and M. Bonanomi, "Ionizing radiation effects on floating gates," *Appl. Phys. Lett.*, vol. 85, no. 3, pp. 485–487, 2004.

[2] G. Cellere, A. Paccagnella, A. Visconti, and M. Bonanomi, "Secondary effects of single ions on floating gate memory cells," *IEEE Trans. Nucl. Sci.*, vol. 53, no. 6, pp. 3291–3297, Dec. 2006.

[3] G. Cellere, A. Paccagnella, A. Visconti, M. Bonanomi, A. Candelori, and S. Lora, "Effect of different total ionizing dose sources on charge loss from programmed floating gate cells," *IEEE Trans. Nucl. Sci.*, vol. 52, no. 6, pp. 2372–2377, Dec. 2005.

[4] A. Gasperin, A. Cester, N. Wrachien, A. Paccagnella, V. Ancarani, and C. Gerardi, "Radiation-induced modifications of the electrical characteristics of nanocrystal memory cells and arrays," *IEEE Trans. Nucl. Sci.*, vol. 53, no. 6, pp. 3693–3700, Dec. 2006.

[5] A. Cester, A. Gasperin, N. Wrachien, A. Paccagnella, V. Ancarani, and C. Gerardi, "Impact of heavy-ion strikes on nanocrystal non volatile memory cell arrays," *IEEE Trans. Nucl. Sci.*, vol. 53, no. 6, pp. 3195–3202, Dec. 2006.

[6] M. Lisiansky, G. Cassuto, Y. Roizin, D. Corso, S. Libertino, A. Marino, S. A. Lombardo, I. Crupi, C. Pace, F. Crupi, D. Fuks, A. Kiv, E. Della Sala, G. Capuano, and F. Palumbo, "Radiation tolerance of NROM embedded products," *IEEE Trans. Nucl. Sci.*, vol. 57, no. 4, pp. 2309–2317, Aug. 2010.

[7] S. Libertino, D. Corso,, G. Muré, A. Marino, F. Palumbo, F. Principato, G. Cannella, T. Schillaci, S. Giarusso, F. Celi, M. Lisiansky, Y. Roizin, and S. Lombardo, "Radiation effects in nitride read-only memories," *Microelectron. Reliab.*, vol. 50, no. 9–11, pp. 1857–1860, Sep.–Nov. 2010.

[8] B. Eitan, P. Pavan, I. Bloom, E. Aloni, A. Frommer, and D. Finzi, "NROM: A novel localized trapping 2-bit nonvolatile memory cell," *IEEE Electron Device Lett.*, vol. 21, no. 11, pp. 543–545, Nov. 2000.

[9] P. J. McWhorter, S. L. Miller, and T. A. Dellin, "Radiation response of SNOS nonvolatile transistors," *IEEE Trans. Nucl. Sci.*, vol. NS-33, no. 6, pp. 1414–1419, Dec. 1986.

[10] Y. Roizin, R. Daniel, S. Greenberg, M. Gutman, M. Lisiansky, V. Kairys, E. Pikhay, and P. Zisman, "Interface traps and reliability performance of microFlash memory," in *Proc. IEEE Non-Volatile Semicond. Memory Workshop*, 2004, pp. 85–87.

[11] A. Shappir, D. Levy, Y. Shacham-Diamand, E. Lusky, I. Bloom, and B. Eitan, "Spatial characterization of localized charge trapping and charge redistribution in the NROM device," *Solid State Electron.*, vol. 48, no. 9, pp. 1489–1495, Sep. 2004.

[12] T. R. Oldham, "Recombination along the tracks of heavy charged particles in SiO2 films," *J. Appl. Phys.*, vol. 57, no. 8, pp. 2695–2702, Apr. 1985.

[13] D. M. Fleetwood, P. S. Winokur, and J. R. Schwank, "Using laboratory X-ray and cobalt-60 irradiations to predict CMOS device response in strategic and space environments," *IEEE Trans Nucl Sci.*, vol. 35, no. 6, pp. 1497–1505, Dec. 1988.

[14] T. R. Oldham and F. B. McLean, "Total ionizing dose effects in MOS oxides and devices," *IEEE Trans. Nucl. Sci.*, vol. 50, no. 3, pp. 483–499, Jun. 2003.

[15] J. H. Stathis, "Percolation models for gate oxide breakdown," *J. Appl. Phys.*, vol. 86, no. 9, pp. 5757–5766, Nov. 1999.
[16] J. H. Stathis, "Reliability limits for the gate insulator in CMOS technology," *IBM J. Res. Develop.*, vol. 46, no. 2/3, pp. 265–286, Mar./May 2002.
[17] E. Y. Wu, "On the Weibull shape factor of intrinsic breakdown of dielectric films and its accurate experimental determination-Part I: Theory, methodology, experimental techniques," *IEEE Trans. Electron Devices*, vol. 49, no. 12, pp. 2131–2140, Dec. 2002.
[18] J. F. Lawless, *Statistical Models and Methods for Lifetime Data*. New York: Wiley, 1982.
[19] J. Jacquelin, "Inference of sampling on Weibull representation," *IEEE Trans. Electron Devices*, vol. 3, no. 6, pp. 806–808, Dec. 1996.

Domenico Corso received the B.S. degree in electronic engineering from the University of Catania, Catania, Italy.

He is currently with the Istituto per la Microelettronica e Microsistemi, National Council of Research (CNR), Catania.

Sebania Libertino received the Ph.D. degree in physics from the University of Catania, Catania, Italy.

She is currently a Senior Researcher with the Istituto per la Microelettronica e Microsistemi, National Council of Research (CNR), Catania.

Michael Lisiansky received the Ph.D. degree in physics and mathematics from Institute of Semiconductor Physics, Ukrainian Academy of Science, Kiev.

He has more than 30 years of experience in semiconductor device development. For the last ten years, he has been with Tower Semiconductor, Migdal Haemek, Israel.

Yakov Roizin received the Doctor of Science (Dr.Hab.) in physics and mathematics (semiconductors and dielectrics) from Moscow Institute of Electronic Technology (MIET).

For the last 15 years, he has been with Tower Semiconductor, Migdal Haemek, Israel, where he is a TowerJazz Fellow and the Director of Emerging Technologies.

Felix Palumbo received the Ph.D. degree in physics from the University of Buenos Aires, Buenos Aires, Argentina.

He is with the Consejo Nacional de Investigaciones Científicas y Técnicas–Comision Nacional de Energia Atomica, Buenos Aires.

Fabio Principato received the Ph.D. degree in applied physics from the University of Palermo, Palermo, Italy.

Since 2004, he has been an Assistant Professor with the Department of Physics, University of Palermo.

Calogero Pace received the Ph.D. degree from the University of Palermo, Palermo, Italy.

He is currently an Associate Professor of electronics with the Department of Electronics, Computer Science and Systems, University of Calabria, Rende, Italy.

Paolo Finocchiaro received the B.S. degree from the University of Catania, Catania, Italy.

He is currently a Nuclear Physicist and the Head Technologist with the Laboratori Nazionali del Sud, Istituto Nazionale di Fisica Nucleare, Catania, Italy.

Salvatore A. Lombardo received the Ph.D. degree in physics from the University of Catania, Catania, Italy.

He is a Research Manager with the Istituto per la Microelettronica e Microsistemi, National Council of Research (CNR), Catania.